LANGMUIR

pubs.acs.org/Langmuir Article

Compound Drop Shape Analysis with the Neumann Number

Guangle Li,[†] Gabriel Robles Del Hierro,[†] Jimmy Z. Di, and Yi Y. Zuo*

Cite This: *Langmuir* 2020, 36, 7619–7626 Read Online

ABSTRACT: A compound droplet is composed of a traditional pendant drop (PD) or sessile drop (SD) sharing the interface with an immiscible phase of comparable sizes, which could be a solid particle, a gas bubble, or most often another droplet of an immiscible liquid. Over the past decade, the study of compound droplets has attracted increasing attention because of extensive applications in many research fields, such as complex fluids, microfluidics, foam and emulsion, and biomedical applications. Among all technical difficulties in characterizing compound droplets, a central problem in surface science is the prediction of its equilibrium shape, which requires knowledge of complicated boundary conditions. Existing dimensionless groups, such as the Bond number traditionally used to evaluate the shape of PDs and SDs, largely fail in predicting the shape of compound droplets. Here, we propose an alternative Bond number, termed the Neumann number, to characterize the shape of compound droplets. Using three dimensionless groups, that is, the Neumann number, the Bond number, and the Worthington number, we have quantitatively predicted and analyzed the shape of traditional PDs/SDs and various compound droplets, including a PD with a spherical particle suspending at the drop apex, a SD with its apex disturbed by a vertical cylinder, and a spherical SD (no gravity) with its apex disturbed by a fluid lens. It is found that the Neumann number can be readily adapted to quantitatively predict and analyze the shape of PDs/SDs and compound droplets.

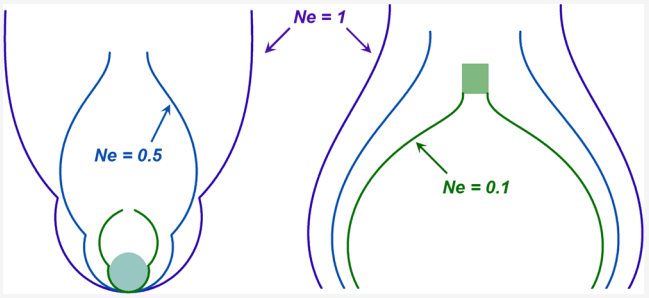

INTRODUCTION

A compound droplet is composed of a traditional pendant drop (PD) or sessile drop (SD) sharing the interface with an immiscible phase of comparable sizes, which could be a solid particle,[1,2] a gas bubble,[3] or most often another droplet of an immiscible liquid.[3−5] Over the past decade, the study of compound droplets has attracted increasing attention because of their extensive applications in many research fields, such as microfluidics,[6−8] foam and emulsion,[9] and biomedical applications.[10,11] Among all technical difficulties in studying compound droplets, a central problem in surface science is the accurate prediction of the equilibrium shape of a compound droplet, which requires knowledge of complicated boundary conditions.[2,3]

Accurately predicting the equilibrium shape of a droplet is the foundation of developing drop shape analysis methodologies for determining surface and interfacial tensions.[12,13] It is generally accepted that the shape of a well-deformed pendant/sessile droplet under the equilibrium or moderately oscillatory conditions slower than 1 Hz can be well predicted by the force balance, as described by the classical Laplace equation of capillary,[14,15] which can be readily solved by axisymmetric drop shape analysis (ADSA).[13,16] Although ADSA has become a standard method for measuring surface/interfacial tension from the shape of a simple PD or SD, its generalization to study compound droplets has been proven to be challenging, largely due to the lack of reliable methods for predicting the shape of compound droplets.

Shape analysis of compound droplets can find many applications in complex fluids and biomedical applications. To give an example, compound drop shape analysis can be an ideal technique for determining the *in situ* surface/interfacial tension of liquids in confined geometries, such as the so-called airway surface liquid (ASL). The ASL is a thin layer of aqueous fluid and mucus at the interface between airway epithelial cells and the air space.[17] Surface tensions and interfacial rheological properties of the ASL determine the mucus clearance of inhaled particles or pathogens, and the Marangoni-driven spreading of pulmonary surfactants in the airway.[18,19] Variations of the ASL surface tension likely contribute to the failure of mucus clearance in respiratory diseases, such as chronic obstructive pulmonary disease and cystic fibrosis.[17,20] *In situ* and *in vivo* measurements of the surface tension of ASL have been attempted by analyzing the shape of an oil microdroplet deposited in the airway.[21] However, because of the lack of reliable methods for predicting

Received: April 24, 2020
Revised: June 8, 2020
Published: June 10, 2020

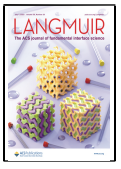

https://dx.doi.org/10.1021/acs.langmuir.0c01216
Langmuir 2020, 36, 7619–7626

the shape of compound droplets, this microdroplet method has only limited success in determining the *in situ* surface tension of ASL.[22]

Another difficulty of studying compound droplets is the lack of a reliable dimensionless parameter to quantitatively analyze the shape of compound droplets. For a simple PD or SD, the equilibrium shape of the droplet corresponds to a Bond number,[23,24] $Bo = \frac{\Delta\rho g L^2}{\gamma}$, where $\Delta\rho$ is the relative density of the droplet, that is, the density difference across the surface or interface, g is the gravitational acceleration, γ is the surface or interfacial tension, and L is the characteristic length representing the size of the droplet. The Bond number can be rewritten $Bo = \left(\frac{L}{c}\right)^2$,[25] where c is the capillary constant of the liquid defined as $c = \sqrt{\frac{\gamma}{\Delta\rho g}}$, and the radius of curvature at the droplet apex (R_0) is commonly used as the characteristic length to determine the Bond number.

Despite being a commonly used parameter for quantifying the drop shape, the Bond number fails to predict droplet deformation under certain circumstances.[25−27] The accuracy of drop shape analysis deteriorates at a low Bond number, and it is well accepted that the small drop volume is the primary source of error in most practical applications. Berry *et al.* introduced a new dimensionless group termed the Worthington number in which the effect of droplet volume was considered to be a primary factor in affecting PD deformation.[26] The Worthington number is defined as $Wo = V/V_{max}$, where V and V_{max} are the actual and the theoretically maximum droplet volumes. The theoretically maximum volume of a PD can be calculated as $V_{max} = \frac{\pi D_t \gamma}{\Delta\rho g}$, where D_t is the diameter of the capillary tube from which the PD is hanging. Hence, the Worthington number can be considered as a modified Bond number with the characteristic length $L = \sqrt{\frac{V}{\pi D_t}}$.[25]

We recently introduced a new dimensionless group called the Neumann number in which the droplet height (H) was considered as an important factor in affecting droplet deformation.[25] The Neumann number is defined as $Ne = \frac{\Delta\rho g R_0 H}{\gamma}$, which can be also considered as a modified Bond number with a characteristic length $L = \sqrt{R_0 H}$. We have demonstrated the advantages of the Neumann number over the Bond number in determining the accuracy of surface/interfacial tension measurements with ADSA.[25]

It is the purpose of the present work to demonstrate the usefulness and advantages of the Neumann number in predicting the shapes of traditional PDs/SDs and previously studied compound droplets. These compound droplets include a PD with a spherical particle (*e.g.*, a ball bearing) suspending at the droplet apex,[1,2] a SD with its apex disturbed by a vertical cylinder (*e.g.*, a fiber or needle),[28,29] and a spherical SD (no gravity) with its apex disturbed by a fluid (gas or liquid) lens.[3] We showed that the Neumann number can be readily adapted to quantitatively predict and analyze the shape of PDs/SDs and compound droplets.

THEORY

Theoretical profiles of the axisymmetric compound droplets were produced by numerical integration of the Bashforth−Adams equations (eq 1) with different boundary conditions.[12]

In these equations, the tangential angle (ϕ), radius (x), and height (z) at any point of the droplet profile are expressed as functions of the arc length (s)

$$\begin{cases} \frac{d\phi}{ds} + \frac{\sin\phi}{x} = \frac{2}{b} + \frac{z}{c^2} \\ \frac{dx}{ds} = \cos\phi \\ \frac{dz}{ds} = \sin\phi \end{cases} \quad (1)$$

where b and c are the radius of curvature and the capillary constant of the droplet, respectively.

Figure 1 shows the coordinate systems of droplets studied in six cases. These are cases A and B: a PD and a SD;[12,25] case C: a PD with a spherical particle suspending at the drop apex;[1,2] case D: a SD with its apex disturbed by a vertical cylinder;[28,29] cases E and F: a SD with its apex disturbed by a fluid lens.[3] Table 1 summarizes the capillary constant (c), radius of curvature (b), and boundary conditions used in solving the Bashforth−Adams equations for cases A−F. It should be noted that the

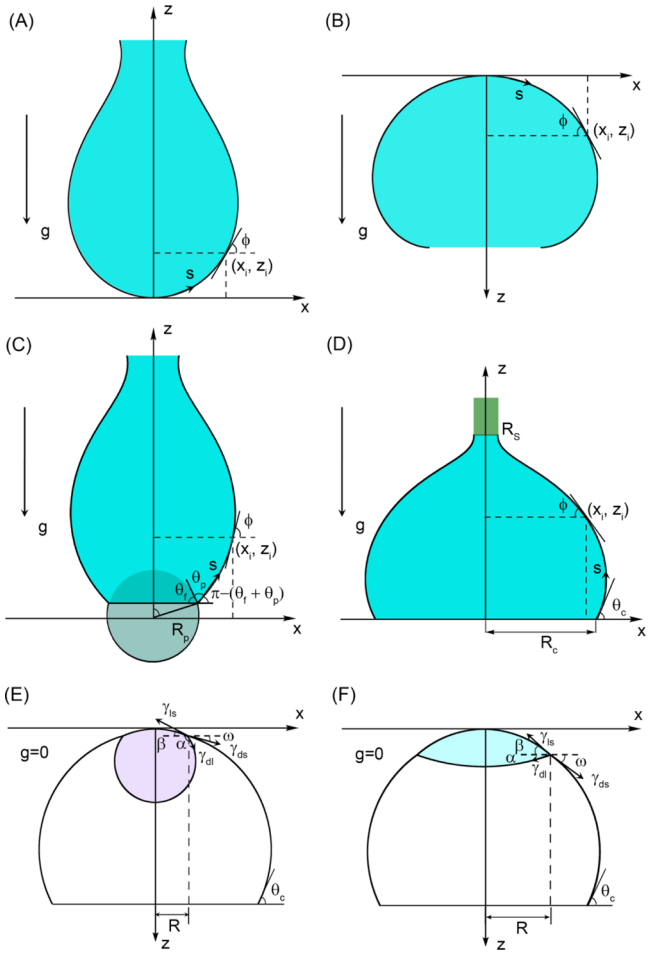

Figure 1. Coordinate systems used in numerical solutions of the Bashforth−Adams equations for axisymmetric compound droplet profiles. (A) PD; (B) SD; (C) PD with a spherical particle suspending at the drop apex; (D) SD with a vertical cylinder disturbing the drop apex; (E) SD with an air bubble floating against the drop apex; (F) SD with a liquid lens resting atop the drop apex. Gravity in (E,F) is set to be zero.

https://dx.doi.org/10.1021/acs.langmuir.0c01216
Langmuir 2020, 36, 7619−7626

Table 1. Capillary Constant (c), Radius of Curvature (b), and Boundary Conditions Used for Solving the Bashforth−Adams Equations in Cases A−F[a]

	cases A and B: PD and SD[12,25]	case C: PD with a suspending particle[1,2]	case D: SD with a vertical cylinder[28,29]	cases E and F: SD with a fluid lens[3]
capillary constant (c)	$\sqrt{\frac{\gamma}{\Delta\rho_d g}}$	$\sqrt{\frac{\gamma}{\Delta\rho_d g}}$	$\sqrt{\frac{\gamma}{\Delta\rho_d g}}$	n/a (negligible gravity)
radius of curvature (b)	R_d	$\sin\theta_f \sin(\theta_f + \theta_p) - \frac{R_p}{R_d}\sin^2\theta_f + \frac{\Delta\rho_d g {R_p}^2}{\gamma}\upsilon(\theta_f) - \frac{\Delta\rho_d g {R_p}^2}{\gamma}\upsilon(\pi) = 0$ $\upsilon(\theta_f) = \frac{(2 - 3\cos\theta_f + \cos^3\theta_f)}{6}$	R_d	$R_{ds} = \frac{R}{\sin\omega}$ $R_{dl} = \frac{R}{\sin\alpha}$ $R_{ls} = \frac{R}{\sin\beta}$
boundary conditions	$x(0) = 0$	$x(0) = R_p \sin\theta_f$	$x(0) = R_c$	$\cos(\alpha + \omega) = \frac{(1 + x^2 - y^2)}{2x}$
	$z(0) = 0$	$z(0) = R_p \cos\theta_f$	$z(0) = 0$	$\cos(\beta - \omega) = \frac{(1 + y^2 - x^2)}{2y}$
	$\varphi(0) = 0$	$\varphi(0) = \pi - (\theta_f + \theta_p)$	$\varphi(0) = \theta_c$	$x = \frac{\gamma_{dl}}{\gamma_{ds}}$, $y = \frac{\gamma_{ls}}{\gamma_{ds}}$
			at $x = R_s$, $z = H$	$V_d = R^3\left[\left(\frac{\sin\theta_c}{\sin\omega}\right)^3 \upsilon(\pi - \theta_c) - \upsilon(\omega) \mp \upsilon(\alpha)\right]$ $V_l = R^3[\upsilon(\beta) \pm \upsilon(\alpha)]$ $\upsilon(\psi) = \frac{\pi}{3}\frac{2 - 3\cos\psi + \cos^3\psi}{\sin^3\psi}$

[a]PD: pendant drop. SD: sessile drop. $\Delta\rho_d = \rho_d - \rho_s$ is the relative density of the droplet, *i.e.*, the density difference between the droplet and the surrounding fluid. γ is the surface tension of the droplet. g is the gravitational acceleration, which was set at 980 cm/s^2. In cases A and B, R_d is the radius of the curvature at the apex of the droplet. In case C, $\Delta\rho_p = \rho_p - \rho_s$ is the relative density of the particle, *i.e.*, the density difference between the particle and the surrounding fluid. R_d is the radius of curvature of the droplet at the contact point with the spherical particle and can be calculated by the force balance on the particle. R_p is the radius of the spherical particle. θ_f and θ_p are the filling angle and the contact angle between the spherical particle and the droplet. These two angles were set at 75 and 60°. $\upsilon(\theta_f)$ is the volume of the spherical cap immersed into the pendant droplet with the filling angle θ_f. In case D, R_d, R_c, and R_s are the mean radius of curvature of the interface at the reference level ($z = 0$), the contact radius with the substrate, and the radius of the vertical cylinder disturbing the drop apex, respectively. θ_c is the contact angle of the droplet on the substrate, which was set at 60°. H is the height of the droplet. In cases E and F, γ_{dl}, γ_{ls}, and γ_{ds} are the surface/interfacial tensions between droplet and lens, lens and surrounding fluid, droplet and surrounding fluid, respectively. R_{dl}, R_{ls}, and R_{ds} are the radii of the interfaces between droplet and lens, lens and surrounding fluid, droplet and surrounding fluid, while α, β, and ω are the angles between these interfaces and the parallel direction at the three-fluid phase contact region. R is the radius of the three-fluid contact region. V_l and V_d are the volumes of the fluid lens and the droplet. The volume of a spherical cap with a base radius R subtending an angle ψ is defined as $V_{cap}(R,\psi) = R^3\upsilon(\psi)$.

mathematical model for cases E and F was initially developed for micron-sized droplets on which the effect of gravity is negligible.[3] Here, we adopt the same model by setting $g = 0$ for mathematical simplicity, although the effect of gravity on millimeter-sized droplets should be significant. Table 2 summarizes the dimensionless groups used to evaluate the drop shapes. These are the Bond number and the Neumann number used in cases A−D, and a modified Worthington number, $Wo = V_l/V_d$, where V_d and V_l are the volumes of the SD and the fluid lens disturbing its apex, used in cases E and F.

RESULTS AND DISCUSSION

Figure 2 shows the theoretical profiles of droplets in the six studied cases. Droplet profiles in cases A−D are shown with increasing Neumann numbers, while droplet profiles in cases E and F are shown with increasing Worthington numbers. For the traditional PD and SD (Figure 2A,B), it can be seen that gradually increasing the Neumann number from 0.01 to 1 predicts a monotonic deformation of the drop shape. It is well known that the accuracy of drop shape analysis in determining surface/interfacial tension depends on droplet deformation. The surface/interfacial tension calculated from a nondeformed nearly spherical droplet can deviate significantly from its true value.[30] Therefore, the Neumann number can be used as a quantitative measure of droplet deformation, and hence a criterion in determining the accuracy of drop shape analysis. In comparison to other parameters for evaluating droplet deformation, such as the Bond number or the purely geometric shape parameter based on the calculation of the total Gaussian curvature,[27,31] the Neumann number has intrinsic advantages of simplicity and straightforward physical meaning. The present study shows that $Ne > 0.5$ may be used as a general criterion for droplet deformation. This observation is in good agreement with

https://dx.doi.org/10.1021/acs.langmuir.0c01216
Langmuir 2020, 36, 7619−7626

Table 2. Bond Number (*Bo*), Neumann Number (*Ne*), and Worthington Number (*Wo*) for Evaluating the Drop Shapes in Cases A−F[a]

dimensionless group	cases A and B: PD and SD	case C: PD with a suspending particle	case D: SD with a vertical cylinder	cases E and F: SD with a fluid lens
Bond number (Bo)	$\frac{\Delta\rho_d g}{\gamma}R_d^2$	$\frac{\Delta\rho_d g}{\gamma}R_p^2$	$\frac{\Delta\rho_d g}{\gamma}R_c R_s$	
Neumann number (Ne)[25]	$\frac{\Delta\rho_d g}{\gamma}R_d H$	$\frac{\sqrt{\Delta\rho_d \Delta\rho_p}\, g}{\gamma}R_p H$	$\frac{\Delta\rho_d g}{\gamma}\frac{R_s R_d H}{R_c}$	
Worthington number (Wo)[25,26]	$\frac{V_d}{V_{max}} = \frac{\Delta\rho_d g}{\gamma}\frac{V_d}{\pi D_t}$			V_l/V_d

[a]PD: pendant drop. SD: sessile drop. $\Delta\rho_d = \rho_d - \rho_s$ is the relative density of the droplet, *i.e.*, the density difference between the droplet and the surrounding fluid. $\Delta\rho_p = \rho_p - \rho_s$ is the relative density of the particle, *i.e.*, the density difference between the particle and the surrounding fluid. γ is the surface tension of the droplet. g is the gravitational acceleration. H is the height of the droplet. In cases A and B, R_d is the radius of the curvature at the apex of the droplet. V_{max} is the theoretical maximum volume for a PD suspended below a capillary tube with the diameter D_t. In case C, R_p is the radius of the spherical particle. In case D, R_d, R_c, and R_s are the mean radius of curvature of the interface at the reference level ($z = 0$), the contact radius with the substrate, and the radius of the vertical cylinder disturbing the drop apex, respectively. In cases E and F, V_l and V_d are the volumes of the fluid lens and the droplet, respectively.

our previous study of the experimental measurement of surface/interfacial tension using ADSA.[25]

Figure 2C shows the compound droplet profiles of a PD with a spherical particle suspending at the drop apex. Because of gravity of the solid particle, an otherwise spherical droplet (such as a small water droplet) can be appreciably deformed. For example, while the PD at $Ne = 0.1$ has a nearly spherical shape (Figure 2A), the compound droplet at $Ne = 0.1$ is significantly deformed by a small suspending stainless steel ball bearing of density 8.02 g/cm^3 and diameter 0.7 mm. Such a compound droplet has been used as a novel droplet configuration for determining the surface/interfacial tension of droplets with very low Bond numbers.[1]

Different from PD/SD, the capillary constant of the compound droplet shown in case C was determined using the geometric mean between the relative densities of the droplet and the particle, that is, $c = \sqrt{\frac{\gamma}{\sqrt{\Delta\rho_d \Delta\rho_p}\, g}}$. The characteristic length of the compound drop was determined using the geometric mean between the particle radius (R_p) and the droplet height (H), that is, $L = \sqrt{R_p H}$. The use of geometric means in evaluating the capillary constant and the characteristic length allows a well-balanced consideration of the effects of both the droplet and the particle on droplet deformation, thus ensuring an ideal dimensionless group $Ne = \frac{\sqrt{\Delta\rho_d \Delta\rho_p}\, g}{\gamma}R_p H$ for evaluating the shape of the compound droplet (Table 2).

The reliability of the Neumann number in evaluating the shape of the compound droplet shown in case C is further demonstrated in Figure 3, which shows the theoretical profiles of the compound droplet with varying size and density of the suspending particle. The contact angle (θ_p) and filling angle (θ_f) between the PD and the suspending particle (Figure 1) were fixed at 60 and 75°, respectively. Figure 3A shows shapes of the compound droplet with a suspending particle of a fixed density $\Delta\rho_p = 2.2$ g/cm^3 and an increasing radius (R_p) from 0.14 to 0.95 mm. With increasing the particle radius and hence increasing Neumann number, the PD is continuously deformed by the suspending particle. Figure 3B illustrates the effect of the particle density (with $R_p = 0.55$ mm) on the shape of the compound droplet. Density of the particle increases from 1.04 to 10.5 g/cm^3, corresponding to the densities of actual materials. It can be seen that with increasing particle density from that of polystyrene to silver, the Neumann number increases from 0.13 to 1. The corresponding profiles of the compound droplet are gradually elongated with the increasing Neumann number. Figure 3C shows the profiles of the compound droplet with simultaneously increasing R_p and $\Delta\rho_p$, while Figure 3D shows the profiles of the compound droplet with increasing R_p but decreasing $\Delta\rho_p$. As shown in Figure 3C, simultaneously increasing the size and density of the suspending particle deforms the droplet much more efficiently than only increasing the size (Figure 3A) or the density (Figure 3B) of the particle. Figure 3D shows that the effects of the size and density of the particle on deforming the droplet balance each other. It appears that the Neumann number successfully predicts the synergistic effects between R_p and $\Delta\rho_p$ on deforming the PD.

Figure 2D shows the compound droplet profiles of a SD with its apex disturbed with a vertical cylinder, such as a fiber or a needle with a radius R_s.[28,29] To determine the corresponding Neumann number, the characteristic length of this compound droplet was determined as $L = \sqrt{\frac{R_s R_d H}{R_c}}$, where R_c is the mean radius of the contact area, and R_d is the radius of curvature at the reference level ($z = 0$). The contact angle (θ_c) of the droplet was fixed at 60°. The Neumann number is $Ne = \frac{\Delta\rho_d g}{\gamma}\frac{R_s R_d H}{R_c}$ (Table 2). It can be seen that the droplet deforms gradually with increasing Neumann numbers in which the radius of the vertical cylinder (R_s) and the drop height (H) play a predominant role in deforming the droplet. This finding is consistent with the previous study, that is, R_s and H are positively correlated to deform the SD, thus increasing the accuracy of surface tension measurements.[28]

To demonstrate the benefit of the Neumann number, Figure 4 shows the theoretical profiles of droplets in cases A−D, with increasing Bond numbers. It can be seen from Figure 4A, the PD at $Bo = 1$ corresponds to the shape of a water droplet of 2.7 mm in the radius of curvature and 7.3 mm in height, significantly larger than the PD at $Ne = 1$, which corresponds to a water droplet with a more realistic size of 1.5 mm in the radius of curvature and 4.9 mm in height (Figure 2A). A similar phenomenon can be found for the SD (Figures 2B *vs* 4B). The size of the SD at $Bo = 1$ is also significantly larger than the SD at $Ne = 1$. For case C, the Bond number fails to predict the

https://dx.doi.org/10.1021/acs.langmuir.0c01216
Langmuir 2020, 36, 7619−7626

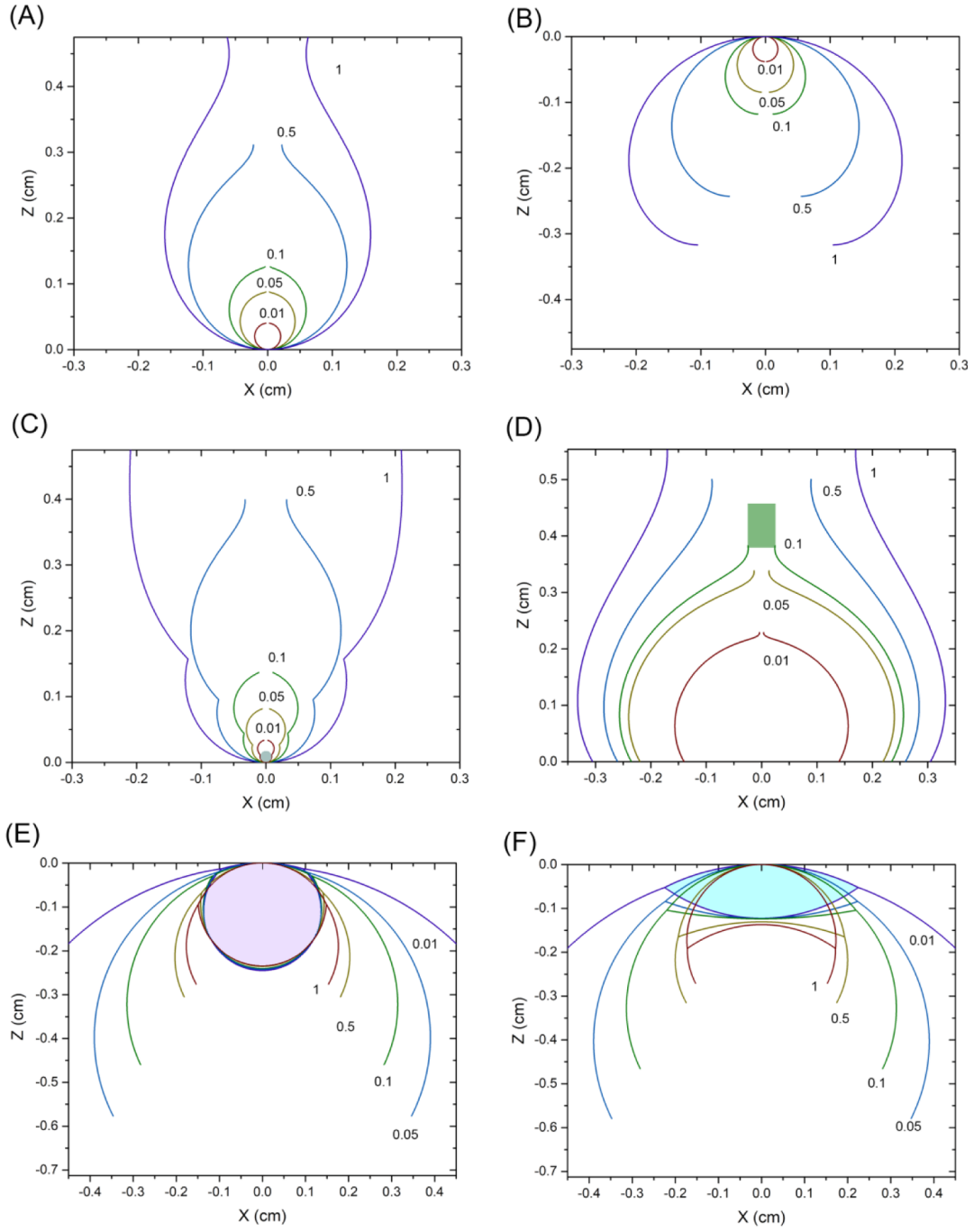

Figure 2. Theoretical profiles of various axisymmetric compound droplets analyzed with the Neumann number (A–D) and the Worthington number (E,F). (A) PD; (B) SD; (C) PD with a spherical particle suspending at the drop apex; (D) SD with a vertical cylinder disturbing the drop apex; (E) SD with an air bubble floating against the drop apex; and (F) SD with a liquid lens resting atop the drop apex. In each case, five droplet profiles are predicted in real physical dimension (cm), corresponding to 0.01, 0.05, 0.1, 0.5, and 1 of the dimensionless groups. (A–D) represent water droplets in air. (E,F) represent perfluorooctane droplets in water. The liquid lens in (F) mimics decane. Gravity in (E,F) is set to be zero.

shape of the compound droplet for $Bo \geq 0.5$, while the Neumann number successfully determines the drop shape for all Neumann numbers between 0.01 and 1 (Figures 2C *vs* 4C). For case D, the benefit of the Neumann number over the Bond number lies in its consideration of the drop height, which is known to play a predominant role in affecting the accuracy of the surface tension measurement using this droplet configuration.[28] Consequently, the Neumann number appears to be a more reliable criterion than the Bond number for predicting and analyzing the shape of traditional PDs/SDs and compound droplets.

Figure 2E,F shows the compound droplet profiles of a SD with a fluid lens, which could be a gas or an immiscible liquid, floating against or resting atop the drop apex, respectively. The volume of the fluid lens was fixed at 10 μL, and the contact angle (θ_c) of the SD was fixed at 60°. For mathematical simplicity, the effect of gravity was set to be negligible ($g = 0$). Hence, the compound droplet profiles in these two cases cannot be evaluated with the Neumann number but using a modified Worthington number $Wo = V_l/V_d$, where V_d and V_l are the volumes of the droplet and the fluid lens, respectively (Table 2).

https://dx.doi.org/10.1021/acs.langmuir.0c01216
Langmuir 2020, 36, 7619–7626

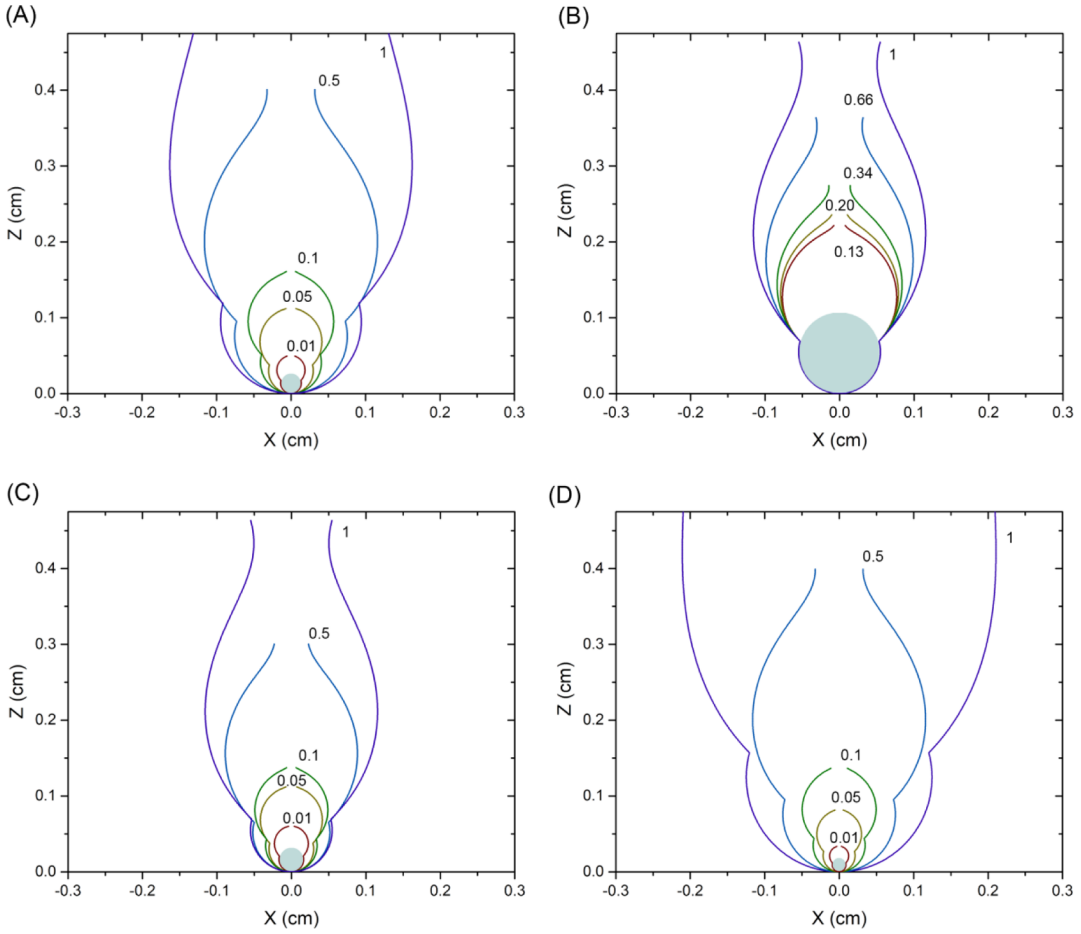

Figure 3. Theoretical profiles of a PD with a spherical particle suspending at the drop apex. (A) Particle of a fixed density of 2.2 g/cm^3 with the increasing radius; (B) particle of a fixed radius of 0.55 mm with the increasing density; (C) simultaneously increasing the radius and density of the particle; and (D) increasing the radius meanwhile decreasing the density of the particle. All theoretical profiles mimic the actual-size (in cm) pendant droplets of water in air. Densities of the particle correspond to actual materials, *i.e.*, 1.04 g/cm^3 for polystyrene, 2.2 g/cm^3 for silica, 4.2 g/cm^3 for titanium, 8.02 g/cm^3 for stainless steel, and 10.5 g/cm^3 for silver.

Generally speaking, the shape of millimeter-sized compound droplets in cases E and F is determined by three sets of physical properties, although the shape of nanometer- and micron-sized droplets can be also affected by the line tension.[32,33] First, the shape of the fluid lens is determined by the balance of surface/interfacial tensions at the three-phase contact line. Formation of the fluid lens requires a negative spreading coefficient, $S = \gamma_{ds} - (\gamma_{dl} + \gamma_{ls})$. The actual shape of the fluid lens is predicted by the Neumann triangle, $\vec{\gamma}_{dl} + \vec{\gamma}_{ds} + \vec{\gamma}_{ls} = 0$,[34] where γ_{dl}, γ_{ds}, and γ_{ls} are surface/interfacial tensions between the droplet and the fluid lens, between the droplet and the surroundings, and between the fluid lens and the surroundings, respectively. A typical example of case E is an air bubble floating against the apex of a perfluorooctane droplet submerged in water. A typical example of case F is a decane lens resting atop of a perfluorooctane droplet submerged in water.

Second, the compound droplet profile is determined by the volume ratio between the fluid lens and the droplet, as predicted by the Worthington number $Wo = V_l/V_d$. As shown in Figure 5A, the fluid lens in case E maintains a biconvex shape. However, as shown in Figure 5B, the fluid lens in case F changes from a biconvex shape to a convex−concave shape when the Worthington number increases beyond a critical value of 0.18. The transition between the biconvex shape and the convex−concave shape is in good agreement with the previous study.[3]

Third, stability of the compound droplet is determined by the relative densities of the droplet, the fluid lens, and the surroundings. Because our current mathematical model prevents us from studying drop stability due to the assumption of negligible gravity, we only briefly discuss the effect of relative densities on compound droplet stability. Most studies reported that a stable compound droplet can be only formed when the fluid lens is lighter than the droplet and the surrounding fluid,[3] which explains the fact that stable oil/water compound droplets in air are rarely observed in reality. However, recent experimental studies demonstrated the formation of stable compound droplets with the surrounding fluid being the least dense phase,[35] and a heavier liquid lens floating atop a lighter droplet with a Worthington number larger than 0.05.[36]

CONCLUSIONS

We have developed a new dimensionless group termed the Neumann number for quantitatively characterizing the shape of compound droplets. Using the Neumann number, the Bond number, and the Worthington number, we have quantitatively predicted and analyzed the shape of traditional PDs/SDs, and various compound droplets, including a PD with a spherical particle suspending at the drop apex, a SD with its apex disturbed by a vertical cylinder, and a spherical SD (no gravity) with its apex disturbed by a fluid lens. It is found that the Neumann

https://dx.doi.org/10.1021/acs.langmuir.0c01216
Langmuir 2020, 36, 7619−7626

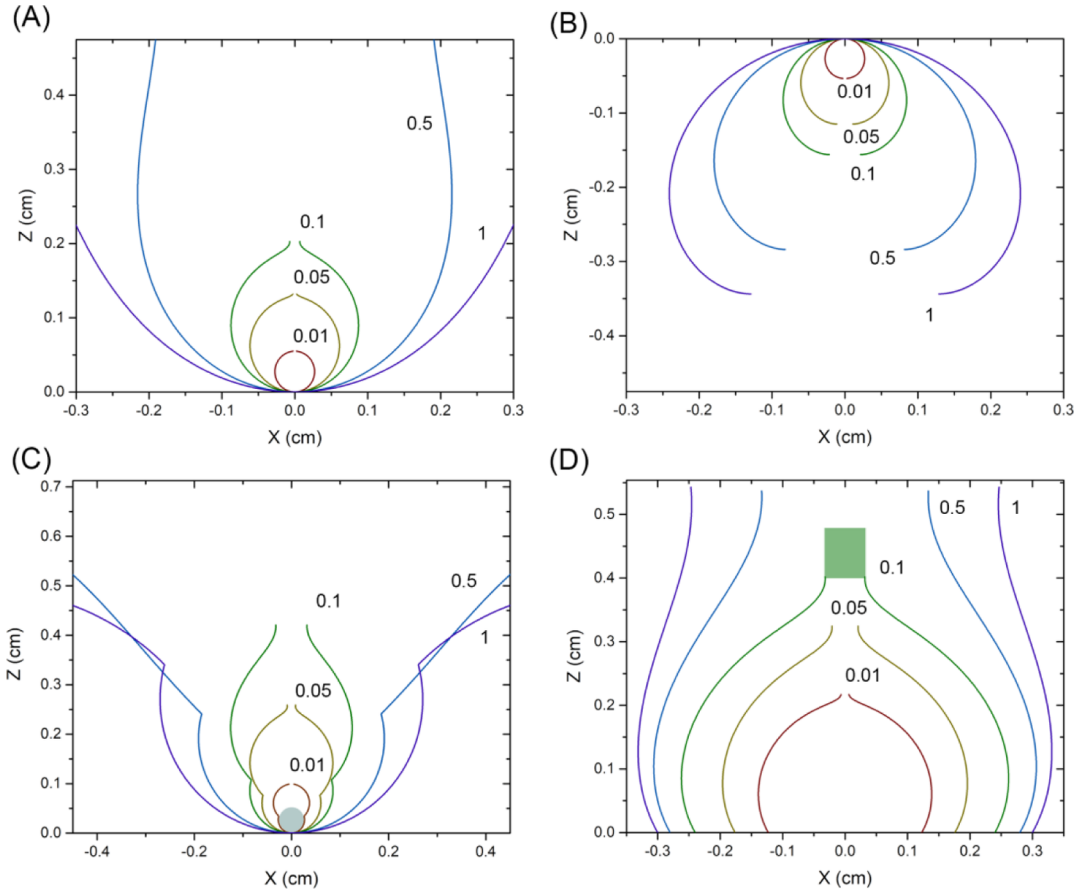

Figure 4. Theoretical profiles of various axisymmetric compound droplets analyzed with the Bond number. (A) PD; (B) SD; (C) PD with a spherical particle suspending at the drop apex; and (D) SD with a vertical cylinder disturbing the drop apex. In each case, five droplet profiles are predicted in real physical dimension (cm), corresponding to 0.01, 0.05, 0.1, 0.5, and 1 of the Bond number.

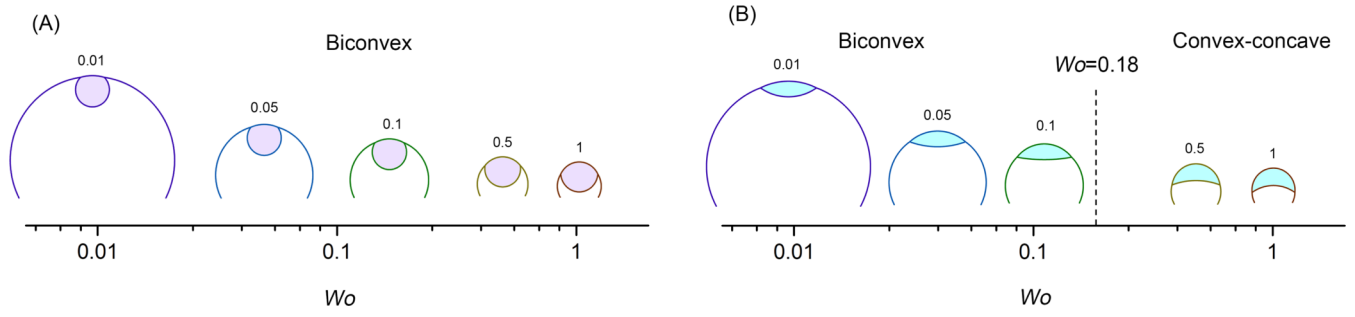

Figure 5. Theoretical profiles of a SD with its apex disturbed by a fluid lens. (A) Air bubble floating against the drop apex at different characteristic Worthington numbers. (B) Liquid lens resting atop the drop apex at different characteristic Worthington numbers. The fluid lens in (A) maintains a biconvex shape, while the fluid lens in (B) changes from a biconvex shape to a convex−concave shape when *Wo* > 0.18. The surface/interfacial tensions between the droplet and the fluid lens, between the droplet and the surroundings, and between the fluid lens and the surroundings are 15.8, 58.5, and 72.0 mN/m in (A), and 7.5, 58.5, and 54.5 mN/m in (B), respectively.

number can be readily adapted to quantitatively predict and analyze the shape of PDs/SDs and compound droplets. Our findings have implications in determining the surface and interfacial tensions of complex fluids using compound drop shape analysis.

AUTHOR INFORMATION

Corresponding Author

Yi Y. Zuo − *Department of Mechanical Engineering, University of Hawaii at Manoa, Honolulu, Hawaii 96822, United States;* orcid.org/0000-0002-3992-3238; Phone: 808-956-9650; Email: yzuo@hawaii.edu; Fax: 808-956-2373

Authors

Guangle Li − *Department of Mechanical Engineering, University of Hawaii at Manoa, Honolulu, Hawaii 96822, United States*

Gabriel Robles Del Hierro − *Department of Mechanical Engineering, University of Hawaii at Manoa, Honolulu, Hawaii 96822, United States*

Jimmy Z. Di − *Department of Mechanical Engineering, University of Hawaii at Manoa, Honolulu, Hawaii 96822, United States*

https://dx.doi.org/10.1021/acs.langmuir.0c01216
Langmuir 2020, 36, 7619−7626

Complete contact information is available at:
https://pubs.acs.org/10.1021/acs.langmuir.0c01216

Author Contributions

†G.L. and G.R.D.H. contributed equally to this work.

Notes

The authors declare no competing financial interest.

■ ACKNOWLEDGMENTS

This work was supported by the National Science Foundation grant no. CBET-1604119 (Y.Y.Z.).

■ REFERENCES

(1) Neeson, M. J.; Chan, D. Y. C.; Tabor, R. F. Compound pendant drop tensiometry for interfacial tension measurement at zero bond number. *Langmuir* **2014**, *30*, 15388−15391.
(2) Neeson, M. J.; Dagastine, R. R.; Chan, D. Y. C.; Tabor, R. F. Evaporation of a capillary bridge between a particle and a surface. *Soft Matter* **2014**, *10*, 8489−8499.
(3) Neeson, M. J.; Tabor, R. F.; Grieser, F.; Dagastine, R. R.; Chan, D. Y. C. Compound sessile drops. *Soft Matter* **2012**, *8*, 11042−11050.
(4) Mahadevan, L.; Adda-Bedia, M.; Pomeau, Y. Four-phase merging in sessile compound drops. *J. Fluid Mech.* **2002**, *451*, 411−420.
(5) Weyer, F.; Ben Said, M.; Hötzer, J.; Berghoff, M.; Dreesen, L.; Nestler, B.; Vandewalle, N. Compound Droplets on Fibers. *Langmuir* **2015**, *31*, 7799−7805.
(6) Utada, A. S.; Lorenceau, E.; Link, D. R.; Kaplan, P. D.; Stone, H. A.; Weitz, D. A. Monodisperse double emulsions generated from a microcapillary device. *Science* **2005**, *308*, 537−541.
(7) Zhou, C.; Yue, P.; Feng, J. J. Formation of simple and compound drops in microfluidic devices. *Phys. Fluids* **2006**, *18*, 092105.
(8) Luo, Z. Y.; He, L.; Bai, B. F. Deformation of spherical compound capsules in simple shear flow. *J. Fluid Mech.* **2015**, *775*, 77−104.
(9) Jaensson, N.; Vermant, J. Tensiometry and rheology of complex interfaces. *Curr. Opin. Colloid Interface Sci.* **2018**, *37*, 136−150.
(10) Kong, F.; Zhang, X.; Hai, M. Microfluidics Fabrication of Monodisperse Biocompatible Phospholipid Vesicles for Encapsulation and Delivery of Hydrophilic Drug or Active Compound. *Langmuir* **2014**, *30*, 3905−3912.
(11) Kan, H.-C.; Udaykumar, H. S.; Shyy, W.; Tran-Son-Tay, R. Hydrodynamics of a compound drop with application to leukocyte modeling. *Phys. Fluids* **1998**, *10*, 760−774.
(12) del Rio, O. I.; Neumann, A. W. Axisymmetric drop shape analysis: Computational methods for the measurement of interfacial properties from the shape and dimensions of pendant and sessile drops. *J. Colloid Interface Sci.* **1997**, *196*, 136−147.
(13) Saad, S. M. I.; Neumann, A. W. Axisymmetric Drop Shape Analysis (ADSA): An Outline. *Adv. Colloid Interface Sci.* **2016**, *238*, 62−87.
(14) Leser, M. E.; Acquistapace, S.; Cagna, A.; Makievski, A. V.; Miller, R. Limits of oscillation frequencies in drop and bubble shape tensiometry. *Colloids Surf., A* **2005**, *261*, 25−28.
(15) Yu, K.; Yang, J.; Zuo, Y. Y. Droplet Oscillation as an Arbitrary Waveform Generator. *Langmuir* **2018**, *34*, 7042−7047.
(16) Neumann, A. W.; David, R.; Zuo, Y. *Applied Surface Thermodynamics*. 2nd ed.; CRC Press: Boca Raton, FL, 2010.
(17) Fahy, J. V.; Dickey, B. F. Airway mucus function and dysfunction. *N. Engl. J. Med.* **2010**, *363*, 2233−2247.
(18) Koch, K.; Dew, B.; Corcoran, T. E.; Przybycien, T. M.; Tilton, R. D.; Garoff, S. Surface Tension Gradient Driven Spreading on Aqueous Mucin Solutions: A Possible Route to Enhanced Pulmonary Drug Delivery. *Mol. Pharm.* **2011**, *8*, 387−394.
(19) Stetten, A. Z.; Iasella, S. V.; Corcoran, T. E.; Garoff, S.; Przybycien, T. M.; Tilton, R. D. Surfactant-induced Marangoni transport of lipids and therapeutics within the lung. *Curr. Opin. Colloid Interface Sci.* **2018**, *36*, 58−69.
(20) Chen, Z.; Zhong, M.; Luo, Y.; Deng, L.; Hu, Z.; Song, Y. Determination of rheology and surface tension of airway surface liquid: a review of clinical relevance and measurement techniques. *Respir. Res.* **2019**, *20*, 274.
(21) Schürch, S.; Bachofen, H.; Possmayer, F. Surface activity in situ, in vivo, and in the captive bubble surfactometer. *Comp. Biochem. Physiol., Part A: Mol. Integr. Physiol.* **2001**, *129*, 195−207.
(22) Zuo, Y. Y.; Veldhuizen, R. A. W.; Neumann, A. W.; Petersen, N. O.; Possmayer, F. Current perspectives in pulmonary surfactant - Inhibition, enhancement and evaluation. *Biochim. Biophys. Acta, Biomembr.* **2008**, *1778*, 1947−1977.
(23) Alvarez, N. J.; Walker, L. M.; Anna, S. L. A non-gradient based algorithm for the determination of surface tension from a pendant drop: Application to low Bond number drop shapes. *J. Colloid Interface Sci.* **2009**, *333*, 557−562.
(24) Berim, G. O.; Ruckenstein, E. Bond Number Revisited: Two-Dimensional Macroscopic Pendant Drop. *J. Phys. Chem. B* **2019**, *123*, 10294−10300.
(25) Yang, J.; Yu, K.; Zuo, Y. Y. Accuracy of Axisymmetric Drop Shape Analysis in Determining Surface and Interfacial Tensions. *Langmuir* **2017**, *33*, 8914−8923.
(26) Berry, J. D.; Neeson, M. J.; Dagastine, R. R.; Chan, D. Y. C.; Tabor, R. F. Measurement of surface and interfacial tension using pendant drop tensiometry. *J. Colloid Interface Sci.* **2015**, *454*, 226−237.
(27) Saad, S. M. I.; Policova, Z.; Acosta, E. J.; Neumann, A. W. Range of validity of drop shape techniques for surface tension measurement. *Langmuir* **2010**, *26*, 14004−14013.
(28) Kalantarian, A.; David, R.; Chen, J.; Neumann, A. W. Simultaneous measurement of contact angle and surface tension using axisymmetric drop-shape analysis-no apex (ADSA-NA). *Langmuir* **2011**, *27*, 3485−3495.
(29) Kalantarian, A.; David, R.; Neumann, A. W. Methodology for High Accuracy Contact Angle Measurement. *Langmuir* **2009**, *25*, 14146−14154.
(30) Saad, S. M. I.; Policova, Z.; Neumann, A. W. Design and accuracy of pendant drop methods for surface tension measurement. *Colloids Surf., A* **2011**, *384*, 442−452.
(31) Saad, S. M. I.; Neumann, A. W. Total Gaussian curvature, drop shapes and the range of applicability of drop shape techniques. *Adv. Colloid Interface Sci.* **2014**, *204*, 1−14.
(32) Amirfazli, A.; Kwok, D. Y.; Gaydos, J.; Neumann, A. W. Line Tension Measurements through Drop Size Dependence of Contact Angle. *J. Colloid Interface Sci.* **1998**, *205*, 1−11.
(33) Law, B. M.; McBride, S. P.; Wang, J. Y.; Wi, H. S.; Paneru, G.; Betelu, S.; Ushijima, B.; Takata, Y.; Flanders, B.; Bresme, F.; Matsubara, H.; Takiue, T.; Aratono, M. Line tension and its influence on droplets and particles at surfaces. *Prog. Surf. Sci.* **2017**, *92*, 1−39.
(34) Aveyard, R.; Clint, J. H. Liquid lenses at fluid/fluid interfaces. *J. Chem. Soc., Faraday Trans.* **1997**, *93*, 1397−1403.
(35) Zhang, Y.; Chatain, D.; Anna, S. L.; Garoff, S. Stability of a compound sessile drop at the axisymmetric configuration. *J. Colloid Interface Sci.* **2016**, *462*, 88−99.
(36) Iqbal, R.; Dhiman, S.; Sen, A. K.; Shen, A. Q. Dynamics of a Water Droplet over a Sessile Oil Droplet: Compound Droplets Satisfying a Neumann Condition. *Langmuir* **2017**, *33*, 5713−5723.